

The Electrostatic Sheet Model for a Plasma and its Modification to Finite-Size Particles

JOHN M. DAWSON

PRINCETON UNIVERSITY
PLASMA PHYSICS LABORATORY
PRINCETON, NEW JERSEY

I. Introduction	1
II. The Electrostatic Sheet Model	2
A. The One-Species Model	3
B. The Numerical Method for Following the Motion of the One-Species, One-Dimensional Plasma	4
C. Numerical Methods for Solving the Two-Species Sheet Model	7
D. Noise and Collisional Phenomenon for the Sheet Model	10
E. Collisional Emission and Absorption of Longitudinal Waves	14
III. Investigations with Finite-Size Particles	16
A. The Finite-Size Particle Model	17
B. Investigation of Fluctuations about Thermal Equilibrium	22
C. The Weak Cold Beam for Finite-Size Particles	24
D. Use of Different Size Charges on the Particles	26
References	27

I. Introduction

ONE OF THE OLDEST and most versatile of the one-dimensional models for numerical investigation of plasmas is the sheet model. This model was first used to investigate electrostatic effects, plasma oscillations, the kinetics of one-dimensional plasmas, and the two-stream instability (Buneman, 1959; Dawson, 1962a, 1962b; Smith and Dawson, 1963; Eldridge and Feix, 1962). In this paper, we will discuss the electrostatic sheet model. The emphasis will be on the methods used to handle these problems on the computer and on a number of problems that are encountered (for example, noise). However, actual codes will not be given.

More recently, the sheet model has been modified by allowing motion in the plane of the sheets, as well as perpendicular to them (Hasegawa and Birdsall, 1964; Shanny *et al.*, 1962; Langdon and Dawson, 1967). This modification allows the inclusion of magnetic effects and the inclusion of

Fokker-Planck-type collisional effects (by a Monte Carlo method). With these modifications, cyclotron waves (Hasegawa and Birdsall, 1964), radiation effects (Langdon and Dawson, 1967), and Harris-type instabilities (Byers and Grewal, 1968) (associated with monoenergetic velocity distributions) have been studied. While these latter modifications are quite interesting and broad in scope, we shall not deal with them here, since to do them justice would take us too far afield.

II. The Electrostatic Sheet Model

There are two electrostatic sheet models, the one-species and the two-species models. The one-species model (Dawson, 1962a) considers a plasma composed of a large number of identical charge sheets embedded in a fixed uniform neutralizing background (see Fig. 1). The sheets are all constrained

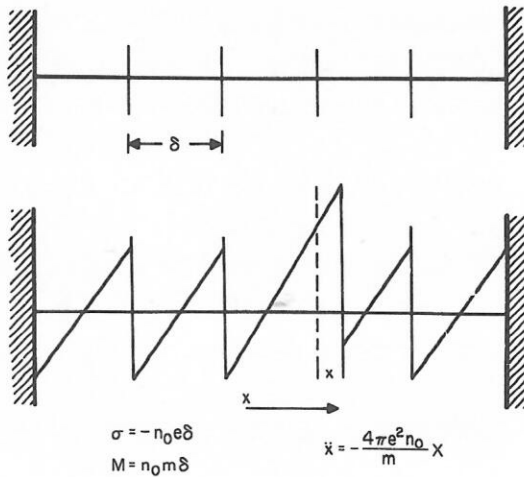


FIG. 1. Sheet model.

to be perpendicular to, say, the x axis, and are allowed to move freely in the x direction. They are allowed to pass freely through each other.

The two-species model (Smith and Dawson, 1963; Eldridge and Feix, 1962) consists of both positively and negatively charged sheets. The sheets are again constrained to be perpendicular to, say, the x axis, and are allowed to move only in the x direction. They are allowed to pass freely through each other. The charges on the sheets are equal and opposite, but their masses are taken to be different. Generally the mass ratio is not taken to be as large as 2000 to 1, because, in that case, the computer spends all its time computing

what the fast-moving electrons are doing. Typically, mass ratios in the range of 10's to 100's are used, and one attempts to scale the results for realistic mass ratios.

We shall begin by discussing the one-species model.

A. THE ONE-SPECIES MODEL

For the one-species model, there exists an equilibrium situation, with the sheets at rest. In this equilibrium situation, the sheets are equally spaced, and the average electric field that a sheet feels is zero, as is shown in Fig. 1. At each sheet, the electric field jumps by $-4\pi\sigma$ (Gauss' law); $-\sigma$ is the charge per unit area. Between the sheets, the electric field varies linearly with distance, due to the background charge. The equilibrium separation of the sheets (δ) is n_0^{-1} , where n_0 is the density of the neutralizing background.

If one of the sheets (say, the i th sheet) is displaced from its equilibrium position by a distance x_i , it passes over an amount of positive charge $\sigma n_0 x_i$ per unit area. By Gauss' law, the electric field which the sheet sees is $4\pi n_0 \sigma x_i$, and its equation of motion is

$$m\ddot{x}_i = -\sigma E = -4\pi n_0 \sigma^2 x_i$$

or

$$\ddot{x}_i = -\omega_p^2 x_i \quad (1)$$

$$\omega_p^2 = 4\pi n_0 \sigma^2 / m.$$

Equation (1) is simply the equation for an harmonic oscillator, and its solution is

$$x_i(t) = x_i(0) \cos \omega_p t + (\dot{x}_i(0)/\omega_p) \sin \omega_p t \quad (2)$$

$$\dot{x}_i(t) = \dot{x}_i(0) \cos \omega_p t - \omega_p x_i(0) \sin \omega_p t. \quad (3)$$

Each sheet oscillates independently of all the others at the plasma frequency.

Equation (1) and the solution given by Eqs. (2) and (3) hold only if the sheet does not cross another. If a crossing does take place, the electric field jumps by $-4\pi\sigma$, and the acceleration undergoes a sudden jump. This situation is the same as if the sheets had interchanged equilibrium positions. Thus, the equation of motion for a sheet is

$$\ddot{x}_i = -\omega_p^2 X_i \quad (4)$$

where x_i is the sheet's position and X_i is its displacement from an instantaneous equilibrium position.

It is now possible to construct a second-one-dimensional plasma model that is entirely equivalent to the one just described. Suppose that, instead of having sheets that pass freely through one another, we had perfectly elastic sheets. It is a property of perfectly elastic collisions between identical particles in one dimension that the particles simply exchange velocities. This leads to the same situation that results from the particles passing through each other. The only difference between the end results is the names we give to the particles.

It is possible to build a mechanical model of the one-dimensional plasma. It consists of a number of identical pendulums, each with an elastic ball at its end. These are lined up and constrained to oscillate only along this line of centers.

One can illustrate a number of properties of one-dimensional plasmas with this model. For example, if the first pendulum is pulled aside and released so as to strike the second, it will give its velocity to the second, the second in turn will give its velocity to the third, and so on. A pulse thus moves through the pendulums. When a pendulum strikes its neighbor it gives up its velocity, but not its displacement. Thus, the pulse leaves the pendulum behind it in a displaced state and they start to oscillate. This is equivalent to the excitation of a plasma oscillation by a fast sheet moving through a plasma.

B. THE NUMERICAL METHOD FOR FOLLOWING THE MOTION OF THE ONE-SPECIES, ONE-DIMENSIONAL PLASMA

We wish to solve Eq. (4) for the sheets, correcting the orbit for crossings of neighboring sheets. When a sheet crosses a neighbor the acceleration jumps by

$$\Delta \ddot{x} = \pm \omega_p^2 \delta \quad (5)$$

where δ is the interparticle spacing, and the + sign is to be used if the sheet crossed was initially on the right, while the minus sign is to be used if it was on the left.

Let the particles be ordered according to their occurrence along x . Now if no crossing takes place, then the solution of Eq. (4) is given by

$$\dot{x}_i(t + \Delta t) = \dot{x}_i(t) \cos \omega_p \Delta t - \omega_p X_i(t) \sin \omega_p \Delta t \quad (6)$$

$$x_i(t + \Delta t) = x_i(t) + \dot{x}_i(t) \sin \omega_p \Delta t - X_i(t)(1 - \cos \omega_p \Delta t). \quad (7)$$

The code computes these noncrossing positions and checks whether any

crossings have taken place; that is, it checks if

$$x_i(t + \Delta t) > x_j(t + \Delta t) \quad \text{for } j > i. \quad (8)$$

(Remember that the particles are ordered in x). If it finds that such a crossing has taken place, it computes the time of crossing by first finding the chords to the two orbit curves in the x, t plane, and then computing the crossing times for these (see Fig. 2). This first approximation to the crossing time, t_{c1} , is given by

$$\Delta t_{c1} = \Delta t \frac{x_j(t) - x_i(t)}{x_j(t) - x_i(t) + x_i(t + \Delta t) - x_j(t + \Delta t)}. \quad (9)$$

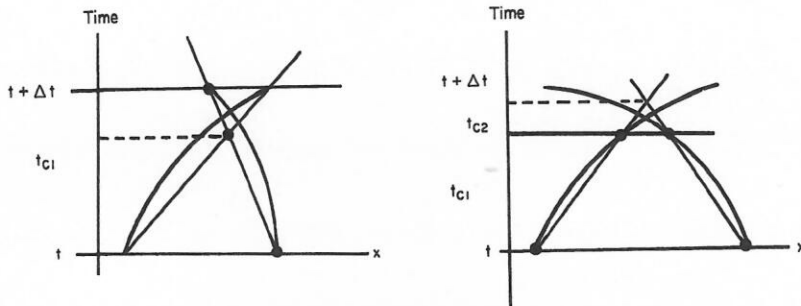


FIG. 2. Crossing figure.

The code next computes the positions of the two particles at this predicted crossing time from the noncrossing orbits. It then computes the chords through the points at t and t_{c1} and finds their crossing time, t_{c2} . This time is used as the correct crossing time. The effect of earlier crossings (if any) during Δt is not included. If two particles crossed before time t , due to corrections to their orbits from crossings in the previous time interval, this t_{c2} will be negative, and the method will find a correction. The orbits of the particles are corrected by adding the constant acceleration $\pm \omega_p^2 \delta$ to their motion over the remainder of the time step, the sign depending on the order of crossing.

The earliest version of this code attempted to calculate the motions without taking into account corrections for crossings during Δt . Even with time steps so short that the probability of one sheet crossing another was small, it was found that the energy drifted down at an unacceptable rate, the rate being roughly

$$(\Delta E/E)_{\text{per } \omega_p^{-1}} = \omega_p \Delta t \quad (10)$$

where Δt is the time step. Not only is this rate rather large, but it improves only as the first power of Δt . By including the first crossing correction, conservation of energy improved as Δt^2 and was about three orders of magnitude better for $\omega_p \Delta t = 0.05$ and $n\lambda_D = 10$. By including the second correction to the crossing time, a further improvement of two orders of magnitude in the energy conservation was obtained for $\omega_p \Delta t = 0.05$ and $n\lambda_D = 10$. The increase in running time due to this last correction was negligible (perhaps 1%) and was more than compensated for by our ability to use larger time steps for a given accuracy.

In addition to energy checks, an old version of the code without the second correction to the crossing time was checked for time reversibility. The motion of a system of 9 sheets was reversed and found to retrace its path within an accuracy of one part in 10^3 (all orbits were this accurate) over a period of 6 oscillations ($\omega_p t = 36$). For this case, there were about 2.5 particles per Debye length.

If the particles are arranged in the order in which they occur in x , then in checking for crossings we need only check nearby particles in the table (hence, nearby particles in x). There is a maximum x separation that particles can have and still cross in a time step. This is given by

$$\Delta x_{\max}(i) = [v_{-\max} + v(i)] \Delta t \quad (11)$$

where $\Delta x_{\max}(i)$ is the maximum distance we must look ahead for a crossing with particles i , $-v_{-\max}$ is the maximum negative velocity of any particle, $v(i)$ is the velocity of the i th particle, and Δt is the time step. We check only ahead (in x) for crossings, since crossings from behind will have been picked up earlier as we move through the table. The maximum negative velocity is updated every ω_p^{-1} .

If this method is to be efficient, the particles must be ordered according to their position in x . This is achieved by counting the number of times a sheet crosses one to its right and subtracting from this the number of times it is crossed by one to its left. This number gives the number of spaces the particle must be advanced (or moved back) in the table. [All tables of pertinent data (positions, velocities, particle identity) are so ordered.] For each crossing a particle experiences from the right, another particle experiences one from the left. Thus, the sum of the total number of crossings (counting those from the right as positive and those from the left as negative) must be zero, and this is used as a check on the codes. Further, this procedure results in a unique ordering for the particles, and no two particles should fill the same place in the table. This is used as a second check on the code.

The boundaries are handled as follows. A set of image charges is included at each end. A sufficient number of these charges is included so that a particle

inside the system cannot overrun the last image particle in one time step. If we desire a reflecting boundary condition, then the image particles are mirror images (equal distance from the boundary, but with negative velocity) of the particles immediately adjacent to the boundary. If we desire periodic boundary conditions, then the images are identical to the particles at the other end of the system except for the fact that they are displaced by plus or minus L (L is the length of the system); the sign depends on which end of the system we are considering. The motions of the last few image particles may not be correct, but this is not important since they are replaced by new images at the end of each time step.

The code is generally run at an average of between one half and one crossing per particle per time step. Energy is conserved to about one part in 10^5 for about 40 time steps if there are 20 particles per Debye length. The code requires roughly 2×10^{-4} sec per particle per time step on an IBM 360/65. Generally, diagnostics such as computation of the velocity distribution function, the Fourier transform of the electric field, and phase space plots for the particles are included. These can consume an appreciable amount of time depending on what is included.

C. NUMERICAL METHODS FOR SOLVING THE TWO-SPECIES SHEET MODEL

The two-species sheet model (Smith and Dawson, 1963) consists of two types of sheets with equal but opposite charges and different masses. These sheets are constrained to be perpendicular to, say, the x axis and are allowed to pass freely through each other.

The equation of motion of a sheet is

$$\ddot{x}_i = (\sigma_i/m_i)E_i \quad (12)$$

where E_i is the average electric field at sheet i (i refers to the order in x). Between crossings, E is a constant, and the orbit of i is given by

$$x_i = x_{i0} + v_{i0}t + \sigma_i E_i t^2/2m_i. \quad (13)$$

Likewise, the orbit of a neighboring particle is

$$x_j = x_{j0} + v_{j0}t + \sigma_j E_j t^2/2m_j \quad (14)$$

where $j = i \pm 1$. Since the charge on a sheet is $\pm\sigma$, by Gauss' law E_j must equal $E_i \pm 4\pi\sigma$, the \pm sign depending on the sign of the charge on i . The crossing time for i and j is obtained by equating x_i and x_j , or is given by

$$(x_{i0} - x_{j0}) + (v_{i0} - v_{j0})t + (\sigma_i E_i/2m_i) - (\sigma_j E_j/2m_j)t^2 = 0. \quad (15)$$

Solving for t gives

$$t = \frac{\Delta v \pm (\Delta v^2 - 4\Delta a \Delta x)^{1/2}}{2\Delta a} \quad (16)$$

where

$$\begin{aligned} \Delta x &= x_{i_0} - x_{j_0}, \\ \Delta v &= v_{i_0} - v_{j_0}, \end{aligned} \quad (17)$$

$$\Delta a = (\sigma_i E_i / 2m_i) - (\sigma_j E_j / 2m_j). \quad (18)$$

It is possible that particles i and j never cross, or that the time of crossing is very large so that they cross other particles in the meantime. However, it is always true that crossing can take place only between instantaneously neighboring particles.

Now we may advance the system, crossing by crossing, recording a particle's position and velocity at the time of its last crossing. We make a list of crossing times for particles crossing their nearest neighbors. The two particles with the shortest crossing times are crossed. After crossing these particles, new crossing times are computed for them with respect to their new neighbors. The old crossing times involving these particles are deleted, and the new crossing times are inserted in the crossing table at the appropriate places.

In order to make the above method efficient so that it does not require a prohibitive amount of computer time, a number of tricks are used. First, the crossing times are inserted in the crossing table in the order in which they occur, so that the next crossing is that one given at the beginning of the table. In order to facilitate entering crossing times in the table, the first few digits of the crossing time are used to address its position in the table. To prevent the need for rearranging the whole crossing table or moving a large number of crossing times in the table when a new one is inserted, the table is made much larger than the total number of crossing times (we used a factor of about 10), so that it contains mostly empty spaces. Thus, when a new crossing time is inserted, it will generally go in an empty space. If there is a crossing time in that space, then it is compared with the one to be inserted, and they are placed in the table in the proper order. If the existing entry must be moved, it will generally be only one space because of the large amount of empty space.

Since we cannot keep an infinitely long crossing table, we must decide on the maximum credible crossing time for neighbors. If the time is longer than this, then one or the other of the particles will be crossed by a third particle before the predicted crossing takes place. The maximum credible crossing

time is determined on the basis of probability arguments. The rate of crossing which a particle with velocity v experiences is roughly

$$n(v^2 + v_T^2)^{1/2} = dN_c/dt = \dot{N}_c \quad (19)$$

where N_c is the number of crossings the particle has experienced, n is the density, and v_T^2 is the mean square random velocity (in this expression we have used the rms velocity relative to other particles in place of the average relative velocity that would apply). Now the probability that the particle does not experience a crossing in a time interval τ is

$$P(\text{no crossing}) = \exp[-\dot{N}_c \tau]. \quad (20)$$

The maximum crossing time kept in the table is chosen so that P is extremely small, generally of the order of 10^{-8} to 10^{-9} . (The minimum value of \dot{N}_c may be used to compute τ ; a τ of the order of twenty times the mean crossing time must be used.) Such a small value of P is required because in a system containing several thousand sheets, each of which makes several thousand crossings during a run, one must ensure that an actual crossing is not overlooked. Because of this, most of the crossing times are concentrated near the top of the table. In order that space be available at the top of the table for insertion of new crossing values, one must take this into account. This situation might be improved by leaving a block of a few spaces at the end of the table to accommodate crossing times greater than 6 or 7 times the average crossing time, but it would complicate the logic for the use and updating of the table and has not been done by us.

As mentioned above, in order to speed the insertion of entries into the crossing table, the first few digits of the crossing time are used as the address. As one proceeds in time the size of the crossing times get larger and larger, and hence the address of the entries become larger and larger. If the crossing table is not to be too large, we must compensate for this. This is done by making the table circular, with the distance around the circle equal to the maximum interval over which a crossing must be considered. A flag is put at the position of the last crossing time considered. This time is subtracted from the new crossing times, and the first few significant figures then determine its location in the table relative to the last crossing.

Boundary conditions are handled by putting image particles at the ends of the system. For reflecting boundary conditions, mirror images of the two end particles are inserted at the mirror points from the two ends. For periodic boundary conditions, images of the opposite ends are inserted at the appropriate locations.

The above method of advancing the system, crossing by crossing, is essentially as accurate as the machine and is quite fast. For the machine used, energy was conserved to ten significant figures over long times ($\omega_p t \approx 100$; the machine has 12 significant figures). The calculation took about one minute per ω_p^{-1} for 1000 electrons and 1000 ions on a CDC 1604, which is several orders of magnitude slower than present fast machines. The calculation time scales like the number of particles times the number of particles per Debye length. The one disadvantage is that a large amount of storage is needed for the crossing table. At the time that the code was written, this was not serious, since the computing time essentially limited the size of the system that could be considered.

It would be possible to use this crossing time method for the one-species problem. One must solve the transcendental equation

$$\delta = (x_i - x_{i+1}) \cos \omega_p t_0 + ([\dot{x}_i - \dot{x}_{i+1}]/\omega_p) \sin \omega_p t_0 \quad (21)$$

in calculating crossing times for neighboring particles (δ equals the inter-particle spacing). On the other hand, it is possible to use the approximate crossing time method used on the one-species model for the two-species model. The latter has been done and works well (it is essentially as fast and conserves energy to about four significant figures over runs with $\omega_p t \approx 100$).

D. NOISE AND COLLISIONAL PHENOMENON FOR THE SHEET MODEL

Because the sheet model consists of discrete particles, a collision-type phenomenon occurs in it. Every time a sheet crosses another, it experiences a jump in the force it feels, and its orbit is changed. These jumps lead to collisional-type effects which may mask the effects one is trying to investigate. If we are to make use of the code, it is important to understand these effects. These effects are also of interest in their own right, as they relate to the kinetic theory of plasmas. Much of this theory can be checked in detail on this model (Dawson, 1962a; 1963; Smith and Dawson, 1963; Eldridge and Feix, 1962; Feix, 1967; Birmingham *et al.*, 1965).

When the standard kinetic theory of plasmas that includes only the two-particle correlation function is applied to the one-species sheet model, it predicts that all stable distribution functions are time-independent. It is relatively easy to understand this result on physical grounds. Consider two identical particles in one dimension which initially have velocities v_1 and v_2 . Let them interact. After this interaction they will have velocities \tilde{v}_1 and \tilde{v}_2 . Now, by conservation of energy and momentum, there are two conserved quantities. The only possible values of \tilde{v}_1 and \tilde{v}_2 that conserve the energy and momentum are

$$v_1 = \tilde{v}_1 \quad v_2 = \tilde{v}_2 \quad (22)$$

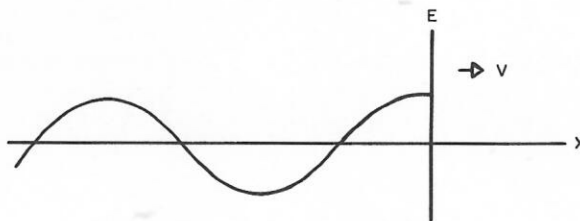
or

$$v_1 = \tilde{v}_2 \quad v_2 = \tilde{v}_1. \quad (23)$$

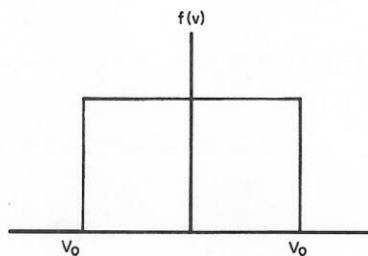
In either case the distribution function is not changed.

One might expect that in a plasma where many particles are interacting simultaneously, these two conservation laws would not contain the whole story. However, the theory treats all interactions as weak, and hence, so far as it is concerned, the effects are additive (assuming uncorrelated or random encounters). The effect of one collision on another is taken negligible, and the conservation relations still freeze the result. Actually, in simultaneous encounters, one encounter affects the other, and so there should be some collisional effect.

These points were checked by a numerical experiment on the one-species sheet model. The actual rate of relaxation to Maxwellian was determined (Dawson, 1963). The problem investigated was that of the time development of a distribution which initially had the square profile shown in Fig. 3. The



Wake of a fast sheet



Initial velocity distribution

FIG. 3. Square $f(v)$.

initial velocity of a particle was obtained by computing a random number that had a uniform probability of lying anywhere between -1 and 1 and then multiplying this number by v_0 . A number of different v_0 's were used to determine the dependence of the time development on the kinetic energy or number of particles per Debye length [$\lambda_D = (v^2)^{1/2}/\omega_p$, $(v^2) = \frac{1}{3}v_0^2$ is the mean square velocity]. The initial positions were chosen to be equally spaced. During the first plasma oscillation, Debye shielding clouds develop around each of the particles. The formation of these clouds requires some energy, and as a result there is a short period of rapid adjustment that rounds off the corners of the distribution. After this initial adjustment, the distribution evolves very slowly. Figure 4 shows the time development of the velocity distribution for the case

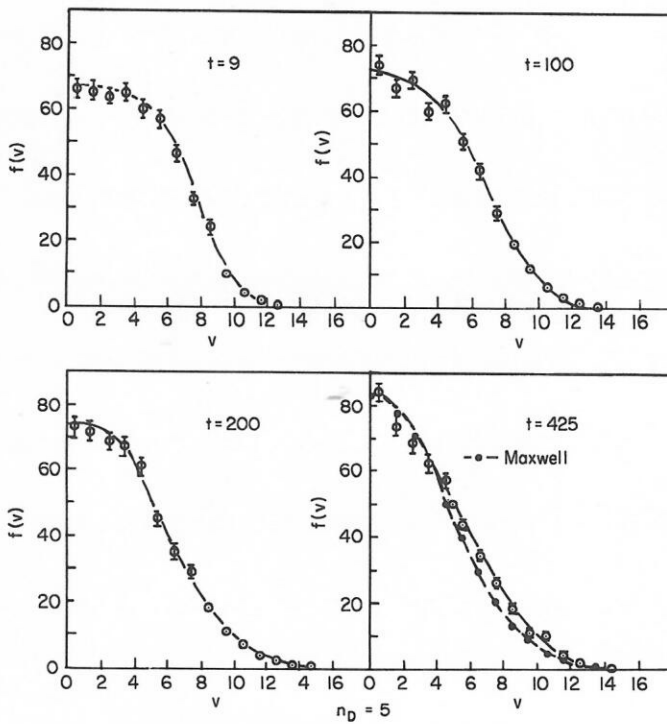


FIG. 4. Time development of π dia.

of 5 particles per Debye length. The first figure shows the situation just after the transient; the other figures show how the distribution evolves toward a Maxwellian. It is essentially reached by $\omega_p t = 425$. This time is much longer than the time required for a group of singled-out particles to acquire the background distribution; this latter time is only $10 \omega_p^{-1}$.

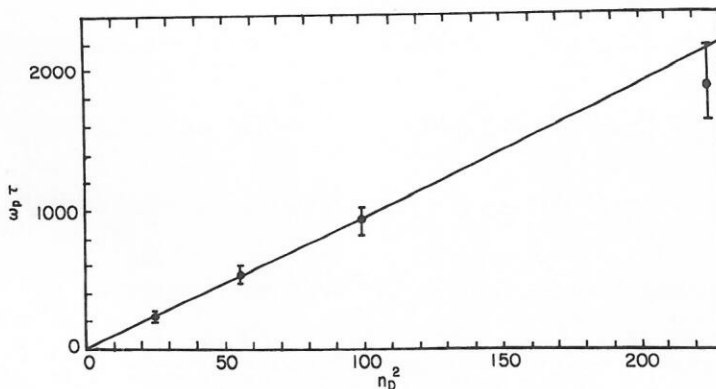
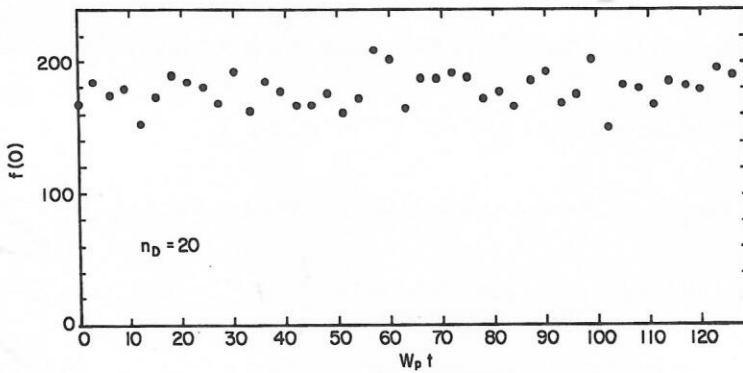
FIG. 5. Relaxation time vs $(n\lambda_D)^2$.

Figure 5 shows a plot of the relaxation time vs $(n\lambda_D)^2$ as determined from such calculations. We see that the relaxation time is proportional to $(n\lambda_D)^2$. This indicates that the simultaneous interaction of three particles gives rise to the relaxation, since the relaxation time due to two-particle interactions would be proportional to $n\lambda_D$ if it did not cancel out. At the present time, there is no theoretical calculation that predicts this relaxation, although it is possible to estimate a relaxation time that is of the right order of magnitude from the emission and absorption of waves by particle encounters.

One interesting point which was found was that the distribution function undergoes rapid random fluctuations about a mean distribution which gradually drifts toward a Maxwellian. The fluctuations in the number of particles with velocities in a small range about zero are shown in Fig. 6. The rapid

FIG. 6. Fluctuation in $f(v)$.

fluctuations are clearly visible. These fluctuations result from the constant exchange of energy between the electric field and the particle kinetic energy. Although this exchange is constantly going on, it is such that it produces very little systematic change. This shows that the fact that the distribution relaxes slowly results from a very subtle balance, and thus the calculation provides an important test of the kinetic theory of plasmas.

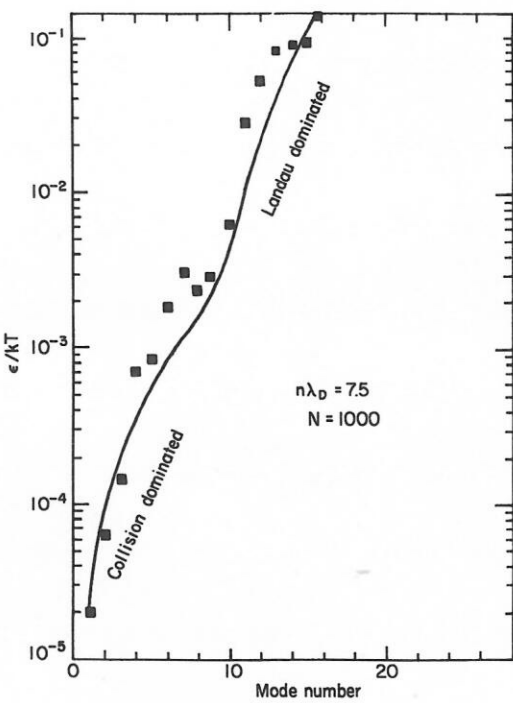
E. COLLISIONAL EMISSION AND ABSORPTION OF LONGITUDINAL WAVES

In the last section we saw that two-particle encounters do not alter the distribution function for a one-species, one-dimensional plasma, and that the actual relaxation of the distribution to a Maxwellian is very slow indeed. One might conclude from this that collisional effects will be of no importance to sheet model calculations. However, this is not so, since collisions can affect one quantity differently from another. During the course of investigations on the sheet model, this was indeed found to be the case. An important example is that of collisional emission and absorption of longitudinal waves.

When two charged particles encounter each other, their mutual acceleration gives rise to the emission of electromagnetic waves. Likewise, the acceleration also leads to the emission of longitudinal waves. This emission of longitudinal waves can also take place in a one-species, one-dimensional plasma.

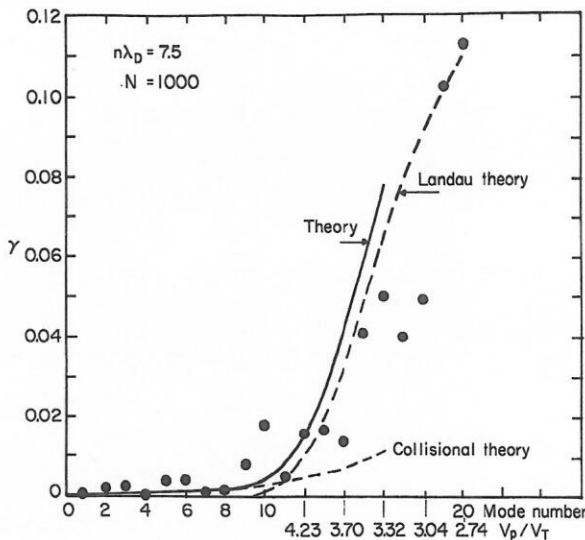
One might ask: If two-particle encounters in the sheet model do not lead to thermalization of a distribution function, how can they lead to the emission and absorption of plasma waves? The answer is the following. The lack of relaxation due to two-particle encounters was a consequence of the conservation of energy and momentum. For the case of emission and absorption of a wave a third element is present—the wave—which also contains energy and momentum, and so the conservation laws no longer fully determine the outcome. A theory for the emission of longitudinal waves has been developed (Birmingham *et al.*, 1965, 1966) which involves the acceleration of two particles and their shielding clouds when they encounter each other. This theory is essentially identical to the theory used to describe weak turbulence in a plasma. Thus, a check of this theory of wave emission also provides a check of weak turbulence theory, at least for the low levels of waves that are encountered here.

The theory for the emission of longitudinal waves was checked on the one-species sheet model (Dawson *et al.*, 1969). The emission encountered here is analogous to that from electron-electron collisions (like particle encounters). Figure 7 shows a plot of the emission *vs* wave number (inverse of the wavelength). The curve is the one predicted by theory. The points are those

FIG. 7. Emissivity *vs* mode number.

obtained from a numerical experiment on a system of 1000 particles with 7.5 particles per Debye length. The agreement is quite good, the emission varying over three orders of magnitude.

Closely related to the emission of waves due to particle encounters is the absorption of waves due to particle encounters. The collisional absorption of waves may be found from the emission because of the fact that the emission and absorption must lead to thermal equilibrium, where each mode of oscillation has an energy kT . Figure 8 shows a plot of the damping time for waves against wave number (number of wavelengths which fit in the system). The system contained 1000 sheets and had 7.5 particles per Debye length. The solid curve is the theoretical one and is the sum of the two dashed curves marked "collisional damping" and "Landau damping." The collisional damping curve is that predicted by the collisional theory just discussed. The damping that is shown in the curve labeled Landau damping does not have its origin in collisions, but rather arises from the absorption of energy by particles moving at the phase velocity of the wave.

FIG. 8. Damping *vs* mode number.

III. Investigations with Finite-Size Particles

In order to overcome the collisional effects associated with sheets, some alternate models would be useful. Basically, we are not interested in the detailed particle motions, but rather in the gross collective motions which involve many degrees of freedom. It should be possible to model a plasma in such a way that we correctly treat its gross behavior while eliminating the detailed behavior associated with particle encounters.

There have been a number of attacks on this problem. The one which might seem the most straightforward is to solve the Vlasov equation numerically. This has been done and with some success (Kellogg, 1965; Armstrong, 1967; Feix and Grant, 1967; Berk and Roberts, 1967). However, there is a basic difficulty which limits all such approaches to following the motion for a finite time (Armstrong, 1967; Berk and Roberts, 1967). The Vlasov equation really describes a system with an infinite number of degrees of freedom (an infinite number of particles). As long as the distribution function has a relatively simple form, so that it can be described by a few parameters, one can follow its development. However, if the distribution function develops a complex structure so that a large number of parameters (of the order of a few thousand) are required, then the finite size of the computer again becomes a constraint, and we can no longer follow the detailed motion. Since the distribution function generally develops this complex structure (probably for

all cases we are interested in doing numerically), this problem cannot be avoided. When this point is reached one must throw away some of the information (one must simplify the distribution function) in order to proceed. Whatever mathematical method one uses to smooth the distribution function, one is never sure of its physical consequence. Such smoothing is somewhat akin to collisions for the discrete particle model. However, it is entirely numerical in nature, depending on the smoothing procedure, and its effects on the results will require analysis (either theoretically or experimentally).

The particle approach to plasma simulation automatically limits the information the machine must handle to that which is required to specify the particle motion. If the enhanced collisional effects can be sufficiently reduced, then this method offers a natural, and physically appealing, method for such limitation. The remaining collisional effects can be understood and taken into account by physical arguments which are already generally well understood.

A number of authors have reduced the collisional effects by smoothing the field due to the particles (Hockney, 1966; Birdsall and Fuss, 1968; Morse, 1968). Hockney has made such smoothing by dividing r space into a number of cells and then computing the fields as if all the particles in one cell were at its center. He ignores the interaction of particles within one cell with each other, thus cutting off the interaction at small distances. Birdsall (Birdsall and Fuss, 1968) has modified Hockney's method by distributing the charge in a cell on its corners. The particle-in-cell method of Morse (1968) is equivalent to Birdsall's charge sharing.

All these methods use a mathematical prescription for smoothing the potential, and this is roughly equivalent to smoothing out the interaction for close encounters. However, all these methods suffer from the same difficulty as smoothing the distribution function for the Vlasov calculation: the mathematical smoothing procedure introduces effects whose consequences are not completely understood. One can eliminate such doubts only by a detailed investigation of the model's behavior (both theoretically and experimentally).

The gross behavior presumably does not depend in a critical way on the detailed motions of all the particles. It should be determined by a number of macroscopic parameters. The number of such parameters may be large, but it should be much less than the number of particles. If this is not true, then we have no hope of describing the plasma. If this is true then there should be a method for keeping the essential information and eliminating the great mass of details which are unimportant. The particle-in-cell method achieves this by using a finite number of particles and of cells.

A. THE FINITE-SIZE PARTICLE MODEL

We have started another approach to this problem. Since we are primarily

interested in the long-wavelength collective motions of the plasma, we should keep only these modes in the calculation. Thus, we should keep only Fourier modes with wavelengths longer than some minimum wavelengths. This can be done simply by dropping the electric fields for wavelengths shorter than those considered important. Thus, we could take the electric field due to a particle to be given by the finite Fourier sum

$$E(r) = 4\pi\sigma \sum_{k_{\min}}^{k_{\max}} \frac{i\mathbf{k}}{k^2} \exp[i\mathbf{k} \cdot (\mathbf{r} - \mathbf{r}_i)]. \quad (24)$$

Here k_{\max} and k_{\min} are determined by the shortest and longest wavelengths we are interested in, r is the position of the particle, and σ is its charge. Generally k_{\max} should be of the order of λ_D^{-1} where λ_D is the Debye length and k_{\min} is determined by the size of the system; k_{\min} is of the order of R^{-1} , where R is the radius of the system.

Now if we take the electric field to be that given by Eq. (24) then the electric field will have oscillations in it as illustrated in Fig. 9 for the one-

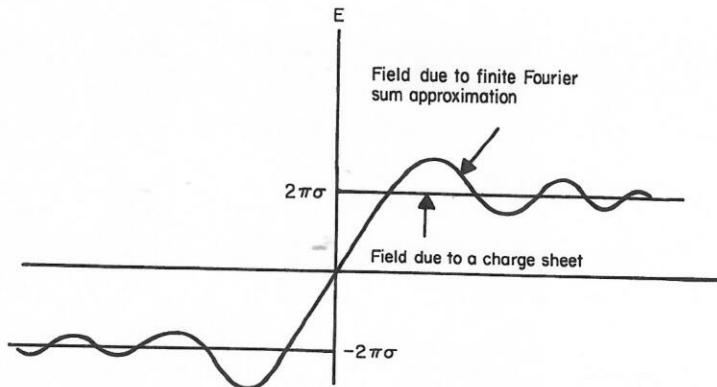


FIG. 9. E field vs x .

dimensional case. Such oscillations of the field are undesirable and can be eliminated (Langdon, 1967). We need not choose the field to be of the form (24) but may take it instead to be of the form

$$E(r) = 4\pi\sigma \sum_{k_{\min}}^{k_{\max}} \frac{i\mathbf{k}}{k^2} f(k) \exp[i\mathbf{k} \cdot (\mathbf{r} - \mathbf{r}_i)] \quad (25)$$

where $f(k)$ is a form factor. One appropriate choice of $f(k)$ is $\exp[-k^2 a^2/2]$. We now recognize that if k_{\max} had been infinite, Eq. (25) would have been the

electric field produced by the Gaussian distribution of charge

$$\rho(r) \propto \sigma \exp[-(r - r_i)^2/2a^2]. \quad (26)$$

Thus, Eq. (26) would be the field due to a finite-size particle of dimensions a . If $k_{\max}^2 a^2$ is large, then all the terms in the infinite sum for k greater than k_{\max} are small, and the finite sum gives an adequate approximation to the field of such a particle. Since the field from such a particle is smooth and does not oscillate, this will be essentially true for the finite sum.

We now restrict ourselves to the one-dimensional case and consider the interaction between particles with charge densities given by

$$\rho(x) = \frac{-\sigma \exp[-(x - x_i)^2/2a^2]}{\sqrt{2\pi a}} \quad (27)$$

where x_i is the position of the center of the cloud and $-\sigma$ is its total charge. Fourier analizing the charge density, we have

$$\rho(k) = \frac{-\sigma \exp[-k^2 a^2/2 + ikx_i]}{\sqrt{2\pi}} \quad (28)$$

while $E(k)$ is given by

$$ikE(k) = \frac{-4\pi\sigma \exp[-(k^2 a^2/2) + ikx_i]}{\sqrt{2\pi}}. \quad (29)$$

The force on particle i due to particle j is given by

$$\begin{aligned} F_{ij} &= \int_{-\infty}^{\infty} E_j(x) \rho_i(x) dx \\ &= \frac{2\sigma^2 i}{\sqrt{2\pi a}} \int dk dx \frac{\exp[ik(x_j - x) - (k^2 a^2/2) - (x - x_i)^2/2a^2]}{k} \end{aligned} \quad (30)$$

$$F_{ij} = 2\sigma^2 i \int \frac{\exp[ik(x_i - x_j) - k^2 a^2]}{k} dk. \quad (31)$$

This force has the same functional form as the E field at x_i due to a particle at x_j with half-width $\sqrt{2a}$ and a charge σ .

Now, since we must work with a finite set of terms, we replace the force

law by the finite Fourier sum

$$F_{ij} = F_0 \sum_{k_{\min}}^{k_{\max}} \frac{\exp[-k^2 a^2]}{k} \sin k(x_j - x_i) \quad (32)$$

where $k = 2\pi n/L$, n is an integer, L is the length of the system. This force is periodic with period L and is equivalent to considering an infinite set of identical systems end to end. The system is overall neutral because the field is periodic. This is equivalent to having a fixed stationary neutralizing background.

The force on particle i due to all other particles is given by

$$F_i = m\ddot{x}_i = \sum_{k_{\min}}^{k_{\max}} \frac{A \exp[-k^2 a^2]}{k} \left\{ \sin kx_i \sum_j \cos kx_j - \cos kx_i \sum_j \sin kx_j \right\} \quad (33)$$

(the i term may be included in the j sums because there is no self-force of i on itself).

To advance the particle in time, we assume that during a time step the force can be computed as if the particles move with a constant velocity. We further assume that $k_{\max} v_i \Delta t$ is small or that a particle moves only a small fraction of the shortest wavelength considered. Thus, we approximate Eq. (33) by

$$\begin{aligned} m\ddot{x}_i = & \sum_{k_{\min}}^{k_{\max}} \frac{A \exp[-k^2 a^2]}{k} \left\{ [\sin kx_i(t)(1 - \frac{1}{2}k^2 v_i^2(t)\tau^2) + kv_i(t)\tau \cos kx_i(t)] \right. \\ & \cdot \left[\sum_j \cos kx_j(t) \right] - [k\tau \sin kx_i(t) + k^2 v_i \tau^2 \cos kx_i(t)] \\ & \cdot \left[\sum_j v_j(t) \sin kx_j(t) \right] - [\frac{1}{2}k^2 \tau^2 \sin kx_i(t)] \cdot \left[\sum_j v_j^2(t) \cos kx_j(t) \right] \\ & - [\cos kx_i(t)(1 - \frac{1}{2}k^2 v_i^2(t)\tau^2) - kv_i(t)\tau \sin kx_i(t)] \cdot [\sum_j \sin kx_j(t)] \\ & - [k\tau \cos kx_i(t) - k^2 v_i(t)\tau^2 \sin kx_i(t)] \cdot \left[\sum_j v_j(t) \cos kx_j(t) \right] \\ & \left. + \frac{1}{2}k^2 \tau^2 \cos kx_i(t) \sum_j v_j^2(t) \sin kx_j(t) \right\}. \end{aligned} \quad (34)$$

Here t is the time at the beginning of a time step and τ is the time elapsed during the time step; only terms up to second order in τ have been kept. Equation (34) can be integrated to yield the velocity and position of the particles.

Equation (34) looks relatively complex, and one may wonder if we are losing rather than gaining by this technique. In this connection we should note the following. First the sums on j are independent of i and can be evaluated for all particles once and for all. Each sum on j must be evaluated for every k considered. Thus if there are N particles and M modes, we must evaluate αNM terms, where α is a constant of proportionality determined by the number of j sums (there are six in this case). Likewise, in advancing the particles we must evaluate βM terms for each particle which gives βMN terms to find. Thus, the time for the whole calculation is proportional to MN . If we had to compute the particle interactions directly (pair by pair), the calculation would be proportional to $N^2/2$. Thus, if M is much smaller than the number of particles, we gain over direct interaction calculations by this technique. In general, we wish to keep only a few modes, the long-wavelength collective modes which are important to the problems under investigation. Thus, M should be much smaller than N . Furthermore, since the particles must represent the full distribution function in phase space, whereas the modes only have to represent the r space part of the disturbance, we need many more particles than modes.

By including the time dependence of the particle positions in Eq. (34), we complicate the calculation. However, by doing this we greatly improve the accuracy of the method and allow ourselves to take larger time steps which more than compensate for the added computation. Without doing this, energy conservation for the system was very poor. By including it we conserve energy to about one part in 10^3 , over times of the order of $100 \omega_p^{-1}$. We have recently found that by using the leap frog method for positions and velocities, much of the advantage of including the time in this expression is obtained.

For the same number of particles and the number of modes as grid points used in the methods of Hockney (1966), Birdsall (1968), and Morse (1968), the above method is slower (their calculation time scales like $\alpha N + \beta M^2$, where M is the number of grid points). However, it is possible to modify this procedure by using a combination of r space and k space grids so as to make the number of computations proportional to $N + \beta M^2$. We have done some preliminary calculations of this type, and substantial time saving is achieved and the accuracy appears to hold up. Since this method involves following exact dynamics of particles interacting through a modified Coulomb potential, many physical checks on the calculations, such as conservation of energy and momentum, can be applied.

B. INVESTIGATIONS OF FLUCTUATIONS ABOUT THERMAL EQUILIBRIUM

The first problem we investigated with the finite-size particle model was the fluctuations about thermal equilibrium to see if they behave as expected. Figure 10 shows a plot of the amplitude of the rms electric field fluctuations *vs*

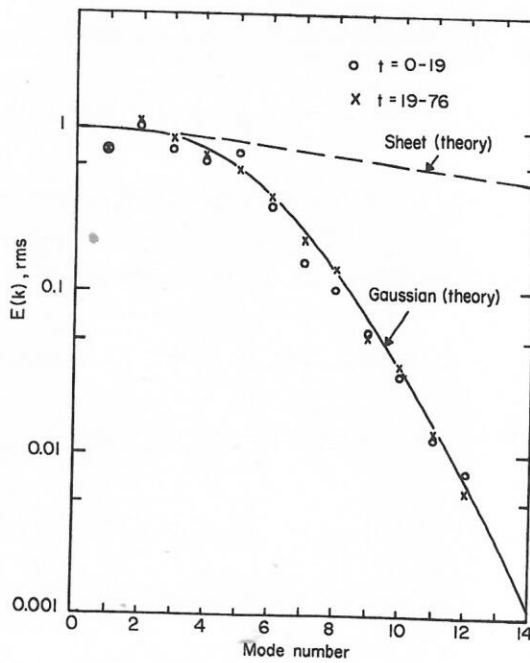


FIG. 10. Rms *E* field *vs* mode number.

mode number for charge clouds with $\alpha = 2\lambda_D$ (λ_D is the Debye length), and with $k_{\max} \lambda_D$ equal to 2. The solid curve is the theoretically predicted curve for Gaussian charge clouds. This curve is predicted from the formula

$$P(E_k) dE_k \propto \exp[-\psi_k(E_k)/KT] dE_k \quad (35)$$

where $P(E_k)$ is the probability of finding the electric field in dE_k about the value E_k , and ψ_k is the work required to create the fluctuations E_k ; ψ_k is given by

$$\psi_k = \frac{E_k^2 L}{16\pi} (1 + k^2 \lambda_D^{-2} \exp[k^2 \alpha^2]). \quad (36)$$

(L is the length of the system.) The first term on the right is the energy in the

electric field, the second term is that required to deform the gas of cloud centers isothermally to the required density fluctuation.

The average value of $E_k^2 L$ obtained from Eqs. (35) and (36)

$$\left\langle \frac{E_k^2 L}{2\pi} \right\rangle = \frac{KT}{2\{1 + k^2 \lambda_D^2 \exp[k^2 a^2]\}}. \quad (37)$$

We see that $\langle E_k^2 \rangle$ is strongly reduced if $k^2 a^2$ is greater than one.

The upper dashed curve in Fig. 10 is that predicted for sheets, i.e., a equals zero. The points are those obtained from the numerical experiment. They agree quite well with the theoretically predicted values. There are some deviations for small mode numbers, but this is most likely due to the fact that the initial conditions do not start these modes out with energy KT , and they take a long time to relax to their thermal value (the averages used here are time averages). As can be seen from Fig. 10, the theoretical fluctuations at long wavelength are hardly affected by the use of finite-size particles, while those at short wavelengths are strongly suppressed as expected. We have run other cases with different values of a and always find similar agreement.

Another interesting thing we can do is derive the dispersion relation for the finite-size particle model. The collisionless Boltzmann equation for these particles is given by

$$\frac{\partial f}{\partial t} + v \frac{\partial f}{\partial x} + \frac{F}{m} \frac{\partial f}{\partial v} = 0 \quad (38)$$

where $f(x, v)$ is the distribution function of cloud centers and velocities. The force on the particles is obtained by integrating $E(\xi)\rho(\xi, x)$ over ξ , x is the position of the center of the charge cloud,

$$F(x) = 4\pi\sigma^2 i \int \frac{dk \exp[-ikx - k^2 a^2]}{\sqrt{2\pi k}} \int f(k, v) dv. \quad (39)$$

This is the same expression one obtains for point particles except for the factor $\exp[-k^2 a^2]$. If we linearize Eq. (38) and Fourier analyze Eqs. (38) and (39) in space and time, we obtain

$$f(k, \omega) = \frac{iF(k, \omega) \partial f_0 / \partial v}{m(\omega + kv - ie)} \quad (40)$$

$$kF = 4\pi\sigma^2 \exp[-k^2 a^2] \int f(k, v) dv. \quad (41)$$

Here ε is a small damping which has been added to determine the direction of integration around the poles. Substituting Eq. (40) into Eq. (41) we obtain the dispersion relation

$$1 = \frac{4\pi\sigma^2}{mk} \exp[-k^2a^2] \int \frac{\partial f_0/\partial v \, dv}{(\omega + kv - i\varepsilon)}. \quad (42)$$

This is the same as the usual dispersion relation except for the factor $\exp[-k^2a^2]$. Thus, the long-wavelength modes are unaffected, while the short-wavelength modes are strongly modified.

C. THE WEAK COLD BEAM FOR FINITE-SIZE PARTICLES

The second problem we investigated was the instability caused by a weak cold beam passing through a warm plasma. For this experiment, systems containing 1000 particles were used; one fifth of them were in the beam. There were twenty particles per Debye length, the beam was cold and had a velocity of four times thermal velocity (the velocities of all particles are shifted so there is no net current). Runs were made with particles of one half, one, and

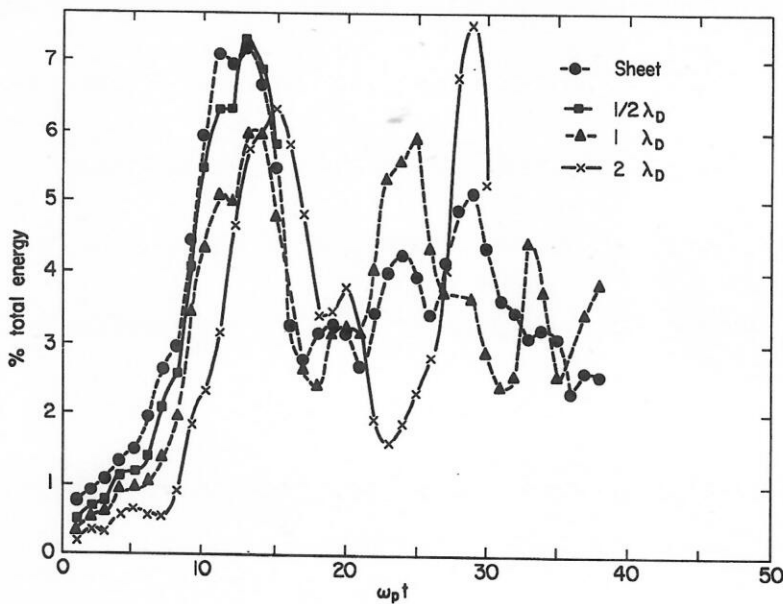


FIG. 11. Electric field energy for two stream instability; comparison for different size particles.

two Debye lengths for their half-widths ($a = 1/2 \lambda_D, \lambda_D, 2\lambda_D$). For all three runs, the initial positions and velocities were the same. A short run was made with the sheet model with identical initial conditions for comparison.

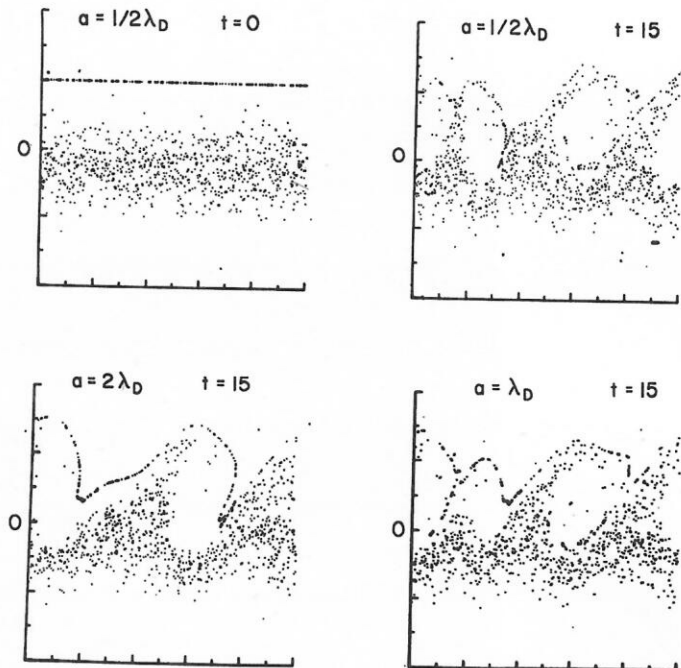
Figure 11 shows plots of the total electric field energy for these four runs. For the sheet case and the $1/2$ Debye length particles, there is quite close agreement. For the one Debye length particles, there is still pretty good agreement though some differences appear. However, an appreciable part of this difference can be attributed to the electric field energy in the short-wavelength modes which are suppressed in this case. A rough correction can be made by adding the initial deviation in electric field energy between the $a = \lambda_D$ case and the sheet case, to the $a = \lambda_D$ case. This will account for about half the difference at the time of the first peak.

When one comes to the two Debye length size particles, a qualitative change takes place, in that the first peak in the electric field energy is appreciably reduced and shifted to a later time, and the second peak is much larger. This difference is probably due to the fact that the size of the particle affects the growth rate of mode three. Table I lists the growth rates for all four cases for modes 1-4.

TABLE I
GROWTH RATES FOR MODES 1-4 VARIOUS
PARTICLE SIZES

a/λ_D	Mode Number			
	1	2	3	4
0	0.163	0.255	0.250	0.148
0.5	0.163	0.255	0.243	0.125
1.0	0.163	0.250	0.220	0.058
2.0	0.162	0.233	0.114	0.002

Figure 12 shows phase space plots of the particle positions for $t = 0$ and $t = 15$. The initial conditions are the same for all cases so that the $t = 0$ plot for $a = \lambda_D/2$ would apply to all cases. The plots for $\lambda_D/2$ and $1\lambda_D$ are strikingly similar, both as to the number of vortexes formed and their shape at $\omega_p t = 15$. For the case of $a = 2\lambda_D$, however, only two vortexes are formed, and thus there is a qualitative difference. This more or less shows that mode three was effectively stabilized by the finite size of the particle, and that this led to the qualitative difference in electric field energy between this case and the others. If more modes had been unstable, say 5 to 10, it is likely that the difference would not have been so great.

FIG. 12. Vortices in XV space.

D. USE OF DIFFERENT SIZE CHARGES ON THE PARTICLES

There is one further modification of this model which we have been investigating. Let us imagine that we have a number of species of particles with charges $-Q_\sigma$ and masses M_σ (σ denotes the species). We take Q_σ/M_σ to be the same for all species. Now the Vlasov equations for this system of particles are

$$\frac{\partial f_\sigma}{\partial t} + \mathbf{v} \cdot \frac{\partial \mathbf{f}}{\partial \mathbf{r}} - \frac{Q_p}{M_\sigma} \mathbf{E} \cdot \frac{\partial \mathbf{f}_\sigma}{\partial \mathbf{v}} = 0 \quad (43)$$

$$\nabla \cdot \mathbf{E} = -4\pi \left(\sum_\sigma Q_\sigma \int f_\sigma d\mathbf{v} - en_0 \right) \quad (44)$$

where en_0 is a fixed uniform neutralizing background (here we are considering point particles, but the whole analysis could be done almost as easily for finite size particle). Now let us define a new distribution function $F(\mathbf{v})$ by

$$F(\mathbf{r}, \mathbf{v}, t) = \sum_\sigma \frac{Q_\sigma}{e} f_\sigma(\mathbf{r}, \mathbf{v}, t) \quad (45)$$

where e is some basic smallest charge unit considered. If we multiply Eq. (43) by Q_σ/e and sum over all σ , then we obtain

$$\frac{\partial F}{\partial t} + \mathbf{v} \cdot \frac{\partial F}{\partial \mathbf{v}} - \frac{e}{m} \mathbf{E} \cdot \frac{\partial F}{\partial \mathbf{v}} = 0 \quad (46)$$

while Eq. (44) is

$$\nabla \cdot \mathbf{E} = -4\pi \left\{ e \int F d\mathbf{v} - \bar{en}_0 \right\}. \quad (47)$$

These are the usual Vlasov equations for a single species of particles. At the Vlasov level, the system behaves the same as a single species plasma.

Now the advantage of using such a system is that, in many problems, most of the particles form a background medium which oscillates in response to a few particles (for example, a bump in the tail of the distribution function). All the computers time is spent in following the mass of particles which are not doing anything interesting. By the above procedure, we could replace the bulk of the particles by a few hundred particles which have perhaps a charge $100 e$, while the particles in the interesting regions of phase space might be represented by a few thousand particles with charge e . This gives us the equivalent of many more particles. Before this can be done, collisional effects with the massive particles must be reduced to an acceptable value. Collisional effects are, of course, not included in the Vlasov description. This is where the use of finite size particles will greatly help us. This procedure should also be useful in one, two, and three dimensions. We have carried out some preliminary investigations on this method, and they look promising. However, much more work is required to determine its limitations and strength.

ACKNOWLEDGEMENTS

The author is deeply indebted to efforts of many people who made this article possible. He should particularly like to acknowledge the efforts of Dr. C. Smith, who largely developed the two-species code, the efforts of Drs. C. G. Hsi, R. Shanny, and W. L. Kruer, who developed the finite-size particle model and the multispecies charge model, and the efforts of H. Fallon and the Computing Group of the Princeton Plasma Physics Laboratory, without whose help the calculations could not have been performed.

This work was performed under the auspices of the U.S. Atomic Energy Commission Contract No. AT(30-1)-1238.

Use was made of the computer facilities supported in part by National Science Foundation Grant NSF-GP 579.

REFERENCES

- ARMSTRONG, T. P. (1967). *Phys. Fluids* **10**, 1269.
- BERK, H. L., and ROBERTS, K. V. (1967). *Phys. Fluids* **10**, 1595.
- BIRDSSALL, C. K., and FUSS, D. (1968). *Bull. Am. Phys. Soc.* **13**, 283.

- BIRMINGHAM, T., DAWSON, J., and OBERMAN, C. (1965). *Phys. Fluids* **8**, 297.
- BIRMINGHAM, T., DAWSON, J., and KULSTRUD, R. (1966). *Phys. Fluids* **9**, 2013.
- BUNEMAN, O. (1959). *Phys. Rev.* **115**, 503.
- BYERS, J., and GREWAL, M. (1968). *Proc. APS Topical Conf. Numerical Simulation of Plasma*, Sept. Paper D3, University of California, Los Alamos, N.M.
- DAWSON, J. (1962a). *Phys. Fluids* **5**, 445.
- DAWSON, J. (1962b). *Nucl. Fusion*, 1962 Suppl., Part 3, 1033.
- DAWSON, J. M. (1963). *Phys. Fluids* **7**, 419.
- DAWSON, J., SHANNY, R., BIRMINGHAM, T. (1969). *Phys. Fluids* **12**, 687.
- ELDRIDGE, O. C., and FEIX, M. (1962). *Phys. Fluids* **5**, 1307.
- FEIX, M. R. (1967). *Symp. Comp. Simulation Plasma and Many-Body Problems*, NASA SP-152, p. 3. Williamsburg, Virginia, April 19-21.
- FEIX, M. R., and GRANT, F. C. (1967). *Symp. Comp. Simulation Plasma and Many-Body Problems*, NASA Report SP-153, p. 151. Williamsburg, Virginia, April 19-21.
- HASEGAWA, A., and BIRDSALL, C. K. (1964). *Phys. Fluids* **7**, 1590.
- HOCKNEY, R. W. (1966). *Phys. Fluids* **9**, 1826.
- KELLOGG, P. J. (1965). *Phys. Fluids* **8**, 102.
- LANGDON B., and DAWSON, J. (1967). *Symp. Comp. Simulation Plasma and Many-Body Problems*, NASA SP-153. Williamsburg, Virginia, April 19-21.
- LANGSON, A. B. (1967). This was suggested to the author in a private communication.
- MORSE, R. L. (1968). Private communication.
- SHANNY, R. A., DAWSON, J. M., and GREENE, J. M. (1962). *Phys. Fluids* **10**, 1281. ^{This is 1961.}
- SMITH, C., and DAWSON, J. (1963). Princeton University Plasma Physics Laboratory, Report Matt-151.